View metadata, citation and similar papers at core.ac.uk

brought to you by CORE

provided by Harvard University - DASH

NMNAT1 Mutations Cause Leber Congenital Amaurosis

The Harvard community has made this article openly available. Please share how this access benefits you. Your story matters.

Citation	Falk, Marni J., Qi Zhang, Eiko Nakamaru-Ogiso, Chitra Kannabiran, Zoe Kelly, Christina Chakarova, Isabelle Audo, et al. 2012. NMNAT1 mutations cause Leber congenital amaurosis. Nature Genetics 44(9): 1040-1045.
Published Version	doi:10.1038/ng.2361
Accessed	February 19, 2015 12:01:24 PM EST
Citable Link	http://nrs.harvard.edu/urn-3:HUL.InstRepos:10622980
Terms of Use	This article was downloaded from Harvard University's DASH repository, and is made available under the terms and conditions applicable to Other Posted Material, as set forth at http://nrs.harvard.edu/urn-3:HUL.InstRepos:dash.current.terms-of-use#LAA

(Article begins on next page)

NIH Public Access
Author Manuscript
Nat Genet. Author manuscript; available in PMC 2013 March 01.

Published in final edited form as:
Nat Genet. 2012 September ; 44(9): 1040–1045. doi:10.1038/ng.2361.

NMNAT1 mutations cause Leber congenital amaurosis

Marni J Falk[1,2,22], **Qi Zhang**[3,4,22], **Eiko Nakamaru-Ogiso**[5], **Chitra Kannabiran**[6], **Zoe Fonseca-Kelly**[3,4], **Christina Chakarova**[7], **Isabelle Audo**[8,9,10,11], **Donna S Mackay**[7], **Christina Zeitz**[8,9,10], **Arundhati Dev Borman**[7,12], **Magdalena Staniszewska**[3,4], **Rachna Shukla**[6], **Lakshmi Palavalli**[6], **Saddek Mohand-Said**[8,9,10,11], **Naushin H Waseem**[7], **Subhadra Jalali**[6,13], **Juan C Perin**[14], **Emily Place**[1,3,4], **Julian Ostrovsky**[1], **Rui Xiao**[15], **Shomi S Bhattacharya**[7,16], **Mark Consugar**[3,4], **Andrew R Webster**[7,12], **José-Alain Sahel**[8,9,10,11,17,18], **Anthony T Moore**[7,12,19], **Eliot L Berson**[4], **Qin Liu**[3,4], **Xiaowu Gai**[20,21,23], and **Eric A. Pierce**[3,4,23]

[1]Division of Human Genetics, Department of Pediatrics, The Children's Hospital of Philadelphia and University of Pennsylvania Perelman School of Medicine, Philadelphia, Pennsylvania, USA

[2]Division of Child Development and Metabolic Disease, Department of Pediatrics, The Children's Hospital of Philadelphia and University of Pennsylvania Perelman School of Medicine, Philadelphia, Pennsylvania, USA

[3]Ocular Genomics Institute, Department of Ophthalmology, Massachusetts Eye and Ear Infirmary, Harvard Medical School, Boston, Massachusetts, USA

[4]Berman-Gund Laboratory for the Study of Retinal Degenerations, Department of Ophthalmology, Massachusetts Eye and Ear Infirmary, Harvard Medical School, Boston, Massachusetts, USA

[5]Department of Biochemistry and Biophysics, University of Pennsylvania Perelman School of Medicine, Philadelphia, Pennsylvania, USA

[6]Kallam Anji Reddy Molecular Genetics Laboratory, LV Prasad Eye Institute (LVPEI), Kallam Anji Reddy Campus, LV Prasad Marg, Hyderabad, India

[7]Institute of Ophthalmology, University College of London, London, UK

[8]Institut National de la Santé et de la Recherche Médicale, U968, Paris, France

Correspondence should be addressed to E.A.P. (eric_pierce@meei.harvard.edu).
[22]These authors contributed equally to this work.
[23]These authors jointly directed the project.

URLs

Exome Variant Server, NHLBI Exome Sequencing Project (ESP), http://evs.gs.washington.edu/EVS/; RetNet Retinal Information Network, https://sph.uth.tmc.edu/retnet/; 1000 Genomes Project website, http://www.1000genomes.org/.

Data access. Exome sequence data for family 047 is available at the NCBI Sequence Read Archive, accession SRP013517.

AUTHOR CONTRIBUTIONS

Experiments were designed by Q.Z., M.J.F., X.G. and E.A.P. LCA case samples and controls were provided by I.A., A.D.B., E.L.B., S.B., C.K., M.J.F, S.J., A.T.M., E.P., S.M.-S., J.-A.S., A.R.W. and E.A.P. Pedigrees were compiled by A.D.B., C.C., C.K., S.J. and E.P. Exome sequencing was performed by M.C. Bioinformatic pipeline development was performed by X.G., M.J.F., E.A.P and M.C. Exome data analyses were performed by J.P., X.G., Z.F.-K. and E.A.P. *NMNAT1* sequencing and segregation analyses were performed by I.A., C.C., M.C., Z.F.-K., D.S.M., L.P., R.S., N.H.W., C.Z. and Q.Z. HPLC-based NMNAT enzyme activity assay and NAD^+ content assay development were performed by E.O. with data analysis performed by E.O., M.J.F., E.A.P. and R.X. *In vitro* functional studies were carried out by Q.Z., E.O., J.O., Q.L. and M.S. The manuscript was written by M.J.F., Q.Z., X.G. and E.A.P.

COMPETING FINANCIAL INTERESTS

The authors declare no competing financial interests.

Accession codes. *Homo sapiens NMNAT1* mRNA, NM_022787.

EdSumm (same for AOP and issue):

Eric Pierce, Xiaowu Gai and colleagues identify mutations in *NMNAT1* as a new cause of Leber congenital amaurosis, an early-onset form of retinal degeneration. *NMNAT1* encodes an isoform of nicotinamide mononucleotide adenylyltransferase, which is required for nicotinamide adenine dinucleotide (NAD^+) biosynthesis.

NIH-PA Author Manuscript
NIH-PA Author Manuscript
NIH-PA Author Manuscript

NIH-PA Author Manuscript

NIH-PA Author Manuscript

NIH-PA Author Manuscript

[9]Université Pierre et Marie Curie (UPMC Paris 06), Unité Mixte de Recherche (UMR)_S 968, Institut de la Vision, Paris, France

[10]Centre National de la Recherche Scientifique, UMR_7210, Paris, France

[11]Centre Hospitalier National d'Ophtalmologie des Quinze-Vingts, INSERM-DHOS Centre d'Investigation Clinique 503, Paris, France

[12]Moorfields Eye Hospital, London, UK

[13]Srimati Kanuri Santhamma Centre for Vitreoretinal Diseases, LV Prasad Eye Institute (LVPEI), Kallam Anji Reddy Campus, LV Prasad Marg, Hyderabad, India

[14]Center for Biomedical Informatics, Children's Hospital of Philadelphia, Philadelphia, Pennsylvania, USA

[15]Department of Biostatistics and Epidemiology, University of Pennsylvania Perelman School of Medicine, Philadelphia, Pennsylvania, USA

[16]Centro Andaluz de Biología Molecular y Medicina Regenerativa (CABIMER), Isla de Cartuja, Seville, Spain

[17]Fondation Ophtalmologique Adolphe de Rothschild, Paris, France

[18]Académie des Sciences–Institut de France, Paris, France

[19]Hospital for Children, London, UK

[20]Department of Molecular Pharmacology and Therapeutics, Loyola University Chicago Health Sciences Division, Maywood, Illinois, USA

[21]Center for Biomedical Informatics, Loyola University Chicago Health Sciences Division, Maywood, Illinois, USA

Abstract

Leber congenital amaurosis (LCA) is an infantile-onset form of inherited retinal degeneration characterized by severe vision loss[1, 2]. Two-thirds of LCA cases are caused by mutations in 17 known disease genes[3] (RetNet Retinal Information Network). Using exome sequencing, we identified a homozygous missense mutation (c.25G>A, p.Val9Met) in *NMNAT1* as likely disease-causing in two siblings of a consanguineous Pakistani kindred affected by LCA. This mutation segregated with disease in their kindred, including in three other children with LCA. *NMNAT1* resides in the previously identified LCA9 locus and encodes the nuclear isoform of nicotinamide mononucleotide adenylyltransferase, a rate-limiting enzyme in nicotinamide adenine dinucleotide (NAD^+) biosynthesis[4, 5]. Functional studies showed the p.Val9Met mutation decreased NMNAT1 enzyme activity. Sequencing *NMNAT1* in 284 unrelated LCA families identified 14 rare mutations in 13 additional affected individuals. These results are the first to link an NMNAT isoform to disease and indicate that *NMNAT1* mutations cause LCA.

Inherited retinal diseases such as LCA represent a heterogeneous group of early-onset blindness that are characterized by progressive dysfunction and death of the rod and cone retinal photoreceptor cells[6]. Despite more than 180 different inherited retinal disease genes having already been identified, the genetic etiology for 40–50% of inherited retinal disease cases remains uncertain[7] (RetNet). Additional loci have been identified with as yet unidentified disease genes, such as the LCA9 locus mapped to chromosome 1p36 (ref. 4). Identifying the genetic basis of inherited retinal diseases is essential to guide potential therapies, as highlighted by the recent success of clinical gene therapy trials for *RPE65*-related LCA[8–12]. Here we employed whole exome sequencing in a large consanguineous

NIH-PA Author Manuscript

NIH-PA Author Manuscript

NIH-PA Author Manuscript

Pakistani pedigree, including five children affected with LCA who did not have mutations in known LCA genes.

Two Pakistani siblings, an 11-year-old girl and her 3-year-old brother (Fig. 1a, Family 047, subjects IV-1 and IV-3), initially presented to the Ophthalmology-Genetics Clinic at the Children's Hospital of Philadelphia for evaluation of LCA based on severe vision impairment, congenital nystagmus and no detectable (<10 μV) retinal function by full-field electroretinography (ERG) testing in early infancy (see Supplementary Note for additional clinical details). Both children also had global developmental delay, non-verbal autism with stereotypies, hypotonia with joint hypermobility and dysmorphic facies. Severe to profound bilateral sensorineural hearing loss was present in the 11-year-old proband (IV-1) as well as in her 8-year-old brother (IV-2), who had a normal eye exam and normal development but clinical features of a suspected mucolipidosis (Supplementary Note). Their parents were first cousins who were visually and developmentally normal (Fig. 1a, subjects III-4 and III-5). Notably, the parents' siblings had married one another (Fig. 1a, subjects III-3 and III-6) and together had two children with similar visual and non-verbal autism phenotypes as the proband (subjects IV-7 and IV-8) as well as one child with isolated LCA (IV-6). Clinical genetic diagnostic testing identified a homozygous mutation in *GJB2* (c.71G>A, p.Trp24*) as the cause of sensorineural hearing loss in subject IV-1, but no mutation was identified in any of the known LCA genes (Supplementary Note).

To search for the genetic cause of LCA in this family, we performed whole exome sequencing of the nuclear family of the 11-year-old proband (Fig. 1a, subjects IV-1, IV-2, IV-3, III-4 and III-5). A homozygous mutation of biparental inheritance that was shared by both affected children but not by their sibling with normal visual acuity was postulated to be their most likely mode of LCA disease given known consanguinity. We identified a total of 113 non-synonymous variants in 86 genes that met these criteria (Supplementary Fig. 1). Four of these variants were rare or novel based on dbSNP 132, 1000 Genomes Project data or NHLBI Exome Sequencing Project (ESP) data[13, 14]. The genes harboring these four variants had known retinal expression based on mouse retina RNA-seq analyses[15]. Only one of these variants was predicted to damage protein function by SIFT, Polyphen2 and other programs, which was c.25G>A (p.Val9Met) in *NMNAT1* (refs. 16–20). Sanger sequencing of the c.25G>A variant in *NMNAT1* validated its segregation with the LCA phenotype in the original nuclear kindred and in the proband's similarly affected cousins, including one individual with isolated LCA (Fig. 1a,b). This variant was not present in 501 controls or any public databases[13, 14].

No clearly pathogenic mutations were identified to be the likely cause of developmental delay, non-verbal autism, hypotonia and dysmorphic facies in family members IV-1, IV-3, IV-7 and IV-8. These presentations likely have a separate genetic etiology from the LCA and deafness in this family because individual IV-6 has LCA alone, individual IV-2 has deafness alone and additional *NMNAT1* mutations were identified in individuals with non-syndromic LCA, as described below.

To determine if *NMNAT1* mutations cause LCA in other families, we sequenced *NMNAT1* in 56 LCA probands (evaluated by M.J.F. and E.A.P. at The Children's Hospital of Philadelphia (CHOP) or by E.A.P. and E.L.B. at the Massachusetts Eye and Ear Infirmary (MEEI)). We found rare compound heterozygous mutations in *NMNAT1* that segregated with disease in family 007, in which the proband was a 5-year-old girl with isolated LCA and no family history of disease (Fig. 1c and Table 1). We also identified compound heterozygous variants in *NMNAT1* that segregated with disease in family 053, in which the proband was a 20-year-old man with LCA (Fig. 1d and Table 1). The four *NMNAT1* variants identified in these subjects were not identified in 501 control samples.

NIH-PA Author Manuscript

NIH-PA Author Manuscript

NIH-PA Author Manuscript

To investigate the frequency of *NMNAT1* mutations in LCA, we screened additional patient populations of varying ethnic backgrounds. This included 248 additional probands ascertained at Institut de la Vision in Paris, LV Prasad Eye Hospital (LVPEI) in India and University College London (UCL). These analyses identified homozygous or compound heterozygous mutations in *NMNAT1* in 11 additional LCA families (Table 1 and Supplementary Fig. 2). All of the mutations detected are rare, and all of them with the exception of the one encoding the p.Glu257Lys variant were predicted to be damaging by PolyPhen 2 and/or SIFT (Table 1). None of the *NMNAT1* variants identified in these subjects were identified by Sanger sequencing in 501 control samples. Review of available clinical information for individuals in whom *NMNAT1* mutations were identified as the cause of their LCA (Supplementary Note) indicated that the majority have atrophic macular lesions (Fig. 2).

NMNAT1 encodes a rate-limiting enzyme that generates NAD^+ both in a biosynthetic pathway from nicotinic acid mononucleotide (NaMN) and in a salvage pathway from nicotinamide mononucleotide (NMN) (Supplementary Fig. 3)[21]. Three functionally non-redundant mammalian NMNAT isoforms encoded by different genes have been identified within distinct cellular compartments, where NMNAT1, NMNAT2 and NMNAT 3 localize, respectively, to the nucleus, Golgi complex and mitochondria[5, 22]. The mitochondrial isoform, NMNAT3, regenerates NAD^+ for cellular energetics, whereas NMNAT1 is involved in nuclear NAD^+ homeostasis necessary for both DNA metabolism and cell signaling[5]. Of interest, Nmnat1 is the principle component of the mouse Wallerian degeneration (Wld^S) fusion protein, which also includes a 70 amino acid N-terminal sequence from the Ube4b multi-ubiquitination factor, and has been shown to have neuroprotective activity[23]. *Nmnat1* homozygous knockout mice are embryonic lethal, whereas heterozygous *Nmnat1* knockout mice have normal development[24]. Loss of *nmnat* in *Drosophila* photoreceptors leads to photoreceptor cell degeneration[25].

We assessed the potential deleterious effects of the novel missense variants p.Val9Met, p.Arg66Trp and p.Arg237Cys on the NMNAT1 protein. These altered residues are located in conserved regions of the protein (Supplementary Fig. 4) and are predicted to damage NMNAT1 protein structure and stability by several prediction programs[26, 27]. All three of these mutant proteins showed correct nuclear localization and normal expression levels following expression of recombinant NMNAT1 protein in heterologous cells (Supplementary Fig. 5a,b). In addition, the p.Val9Met mutant protein correctly localized to the nucleus of a fibroblast cell line obtained from the LCA proband in family 047 (Fig. 1a, subject IV-1 and Supplementary Fig. 5c)[22].

Given the normal nuclear localization and expression of the mutant NMNAT1 proteins, we postulated that the deleterious effect of the p.Val9Met, p.Arg66Trp and p.Arg237Cys variants might be on NMNAT1 enzymatic function. We therefore measured the NAD^+ biosynthetic activity of purified recombinant NMNAT1 wild-type and mutant proteins (Fig. 3a). Despite variability in enzyme rates observed between experimental days, the p.Val9Met protein NMNAT1 activity was reproducibly and significantly decreased compared to same-day wild-type values (63.4% median reduction, interquartile range 31.4–88.7 , Wilcoxon rank sum test, $P = 0.0015$). The enzyme activity of the p.Arg66Trp protein was also significantly decreased (99.5% median reduction, interquartile range 0.01–0.11, Wilcoxon rank sum test, $P = 0.0014$). The enzyme activity of the p.Arg237Cys mutant protein showed only marginally reduced activity (by 18.9%, interquartile range 41.1–90.1, Wilcoxon rank sum test, $P = 0.034$) (Fig. 3a), raising the question of how this mutation causes disease. It has been observed that NMNAT1 forms functional homo-oligomers and that amino acids 234–238 participate in these protein interactions[5]. To evaluate whether the pathogenic effect of the p.Arg237Cys variant could relate to its location in a region of NMNAT1 involved in

NIH-PA Author Manuscript

NIH-PA Author Manuscript

NIH-PA Author Manuscript

protein multimerization, we measured NMNAT1 activity in recombinant protein purified from cells co-transfected with constructs for both the p.Arg66Trp and p.Arg237Cys variants that were identified in family 007. We observed notably reduced enzyme activity (to 18% of wild-type control rate; data not shown) in the combined protein preparation. Additional studies using extracts from the p.Val9Met proband's fibroblast cells (Fig. 1a, subject IV-1) showed a decrease in total cellular NMNAT enzyme activity by 73% (two-tailed *t* test $P = 0.016$) relative to wild-type control (Fig. 3b). These data suggest the pathogenic effects of these mutations relate at least in part to significantly reduced NMNAT1 enzyme activity. It will be of interest to investigate the function of the mutant NMNAT1 proteins in retinal cells, given the isolated retinal phenotype of this disease.

The total NAD^+ concentration of human cells has many contributing determinants[21, 28]. We measured NAD^+ in the LCA proband's fibroblast cell line (Fig. 1a, subject IV-1) to determine whether the p.Val9Met variant in the nuclear-localized NMNAT1 protein significantly impacted total cellular NAD^+ content. Fibroblasts from the LCA proband (subject IV-1) showed a 16% decrease in NAD^+ content relative to wild-type controls, although this difference was not significant (two-tailed *t* test $P = 0.067$; Fig. 3c). These data suggest that the reduction in NMNAT1 enzyme activity caused by the p.Val9Met variant may be sufficient to impact total cellular NAD^+ content.

Cellular NAD^+ concentrations can be directly increased by nicotinic acid, which requires NMNAT activity for its conversion to NAD^+ (Supplementary Fig. 3)[29]. We therefore asked whether the cellular NAD^+ levels in the NMNAT1 p.Val9Met mutant fibroblasts (subject IV-1) was altered by treatment with 10 mM nicotinic acid for 24 hours. Importantly, while nicotinic acid significantly increased the total cellular NAD^+ content by 53% in control cells (two-tailed *t* test $P = 0.021$), it had no effect on NAD^+ content of the LCA proband's fibroblasts (Fig. 3c; two-tailed *t* test $P > 0.05$). The failure of nicotinic acid to increase the NAD^+ content in NMNAT1 p.Val9Met mutant fibroblasts provides further evidence that they have a significant deficiency in their cellular NMNAT enzymatic activity.

In summary, we report here the first instance of any disease association with an NMNAT isoform[5]. *NMNAT1* mutations cause LCA and are the likely pathogenic basis for disease previously linked to the LCA9 locus, although the family originally linked to this locus was not available for analysis in this study[4] (Chris Inglehearn, personal communication). Through exome sequencing in a consanguineous Pakistani LCA kindred and subsequent Sanger sequencing of *NMNAT1* in 285 unrelated LCA probands, we identified mutations in 14 unrelated families (14/285 = 4.9 % of unrelated cases). This work suggests that mutations in *NMNAT1* are a relatively common cause of LCA[3]. However, since the cohorts of individuals used for these studies are enriched for subjects without mutations in known LCA disease genes, the proportion of all LCA cases caused by *NMNAT1* mutations is likely to be over-estimated by these data.

The identification of *NMNAT1* as an LCA disease gene raises the intriguing question of how mutations in a widely expressed NAD^+ biosynthetic protein lead to a retina-specific phenotype. The data presented suggest that the retinal degeneration phenotype observed in individuals with *NMNAT1* mutations results from decreased NAD^+ biosynthetic activity. This hypothesis is consistent with findings from studies of the Wld^S protein in mice, which demonstrated that the neuroprotective effect of the Wld^S protein requires both the Ube4b component and an enzymatically active NMNAT1 portion of the chimeric protein[30]. However, it appears that in some systems, such as *Drosophila*, *nmnat* alone has a neuroprotective role that may be independent of its NAD^+ biosynthetic activity[25, 31]. Thus, it remains to be determined if retinal degeneration caused by mutations in *NMNAT1* results primarily from the loss of a potentially novel neuroprotective effect of NMNAT1 or to a

NIH-PA Author Manuscript

NIH-PA Author Manuscript

NIH-PA Author Manuscript

previously unappreciated role of NAD^+-mediated signaling in retinal health and disease. In either case, *NMNAT1* mutations represent a novel pathophysiologic cause of LCA, further underscoring the genetic heterogeneity of inherited retinal diseases[3, 6]. We postulate that pharmacologic and/or genetic therapies directed at restoring cellular NAD^+ homeostasis in retinal cells may offer a therapeutic strategy for *NMNAT1*-related LCA.

ONLINE METHODS

Subject recruitment and clinical evaluations

The clinical study was approved by the institutional review boards of The Massachusetts Eye and Ear Infirmary, Children's Hospital of Philadelphia, CPP Ile de France V, LV Prasad Eye Hospital, and University College London, and conformed to the tenets of the Declaration of Helsinki. Informed consent was obtained from the participants. Complete ophthalmic and clinical genetic evaluations of members of family 047 (subjects IV-1, IV-1, IV-3), family 007 (subject II-2), and family 053 were performed by M.J.F. and E.A.P. in the Ophthalmology-Genetics Clinic at the Children's Hospital of Philadelphia.

Exome sequencing

Exome capture was performed using Agilent Technologies SureSelectXT 50 Mb All Exon Targeted Enrichment Kit as described in the kit manual[36]. The resulting exome capture libraries were 2 × 101 bp paired-end sequenced on an Illumina HiSeq 2000 Next-Generation Sequencing system using v2.5 SBS chemistry with average flowcell lane cluster densities of ~800 K/mm^2. One exome sample was analyzed per flowcell lane to obtain a minimum 10x read depth for 92–95% of the targeted exome.

Exome data analyses

BWA (version 0.5.9-r16) was used to align the sequence reads to the human reference genome GRCh37 downloaded from the 1000 Genomes Project website (http://www.1000genomes.org/)[37]. Samtools (version 0.1.12 or r859) was used to remove potential duplicates (with rmdup command), and make initial SNP and indel calls (with pileup command)[38]. A custom program was developed and used to further refine the SNP and indel calls. The custom program uses a false discovery rate approach to adjust raw base counts at a candidate position after Benjamini and Hochberg correction based on quality values of all bases[39]. A coverage depth cutoff of 10X is then applied. The fraction of a variant base has to be between 0.25–0.75 to be called heterozygous and above 0.75 to be called homozygous. Resulting variant calls were annotated using our custom human bp codon database. This database maps each base position in the human reference genome, based on Ensembl Release 65 gene annotations, to its corresponding, if any, transcripts, genes, codons, encoded amino acids, and translation frames. Additional annotations of each variant call were provided using data sets downloaded from the 1000 Genomes Project website (http://www.1000genomes.org/), the NHLBI Exome Sequencing Project Exome Variant Server (http://evs.gs.washington.edu/EVS/) and the UCSC Genome Browser (http://genome.ucsc.edu/). These annotations include allele frequencies, SIFT and PolyPhen predictions, and phastCons conservation scores[16, 17]. Custom scripts were also developed and used to identify candidate variants that fit different filtering criteria, such as genetic models.

NMNAT1 PCR amplification, Sanger sequencing and genotype confirmation

Subjects in families 007, 047 and probands from other families with LCA were selected for Sanger sequence analysis using primers to amplify all four exons and intron-exon boundaries of *NMNAT1* (Supplementary Table 1). PCR products were sequenced with the

NIH-PA Author Manuscript

NIH-PA Author Manuscript

NIH-PA Author Manuscript

ABI PRISM Big Dye Terminator Cycle Sequencing V2.0 Ready Reaction kit on ABI 3100 or 3730 DNA analyzers (Applied Biosystems). To genotype the members of family 047, the relevant PCR product was digested with AcuI, which cuts the wild-type but not mutant sequence.

Human fibroblast culture and nicotinic acid treatment

Skin biopsies were performed on two siblings with LCA and their parents (Fig 1a, subjects IV-1, IV-3, III-4, III-5) following informed consent per approved CHOP IRB protocol (#08-6177, M.J.F.). Fibroblast cell lines were established in the CHOP CytoGenomics Laboratory, and subsequently maintained in T75 flasks in a 37°C CO_2 incubator per standard protocol in DMEM (Gibco) with 20% FBS, 2 mM L-glutamine, 1 mM pyruvate and 50 μg/mL uridine (Calbiochem). Cells were grown to confluence prior to undergoing functional analyses. Cells were treated in T75 flasks with 10 mM nicotinic acid (Sigma) for 24 hours, trypsinized, washed twice with Hank's Balanced Salt Solution (Gibco), and flash frozen in liquid nitrogen for HPLC analysis.

Cell culture

CHO-K1 and wild-type mIMCD3 cell lines were purchased from American Type Culture Collection (ATCC). The mIMCD3 cells were maintained in DMEM:F12 media supplemented with 10% FBS and 0.5 mM sodium pyruvate. CHO cell culture was performed in F12 medium supplemented with 10% FBS. Transfection was performed with Lipofectamine 2000 (Invitrogen) and cells were processed for immunocytochemistry 48–72 h after transfection. Human skin fibroblast cells obtained from two LCA siblings (Fig 1a, subjects IV-1 and IV-3) and their parents (Fig 1a, subjects III-IV and III-V) were maintained in Medium 106 (Invitrogen) with low serum growth supplement, and grown to confluence prior to undergoing immunofluorescence and immunoblot analyses.

Immunofluorescence analyses

Cells were fixed in 4% paraformaldehyde, permeabilized, and then blocked with 1% bovine serum albumin (BSA) and 0.2% Triton X-100 in PBS, as previously described[40]. The cells were then stained with anti-V5 antibody (Invitrogen) followed by Alexa Fluor 555–conjugated goat anti-mouse IgG (Invitrogen)[40]. Fluorescent signals were visualized using a Nikon Eclipse fluorescent microscope.

Western blotting

Total cell lysates from CHO cells transfected with pCAG V5-*NMNAT1*-IRES-EGFP plasmid were separated on a precast NuPAGE 4–12% Bis-Tris Gel (Invitrogen) and transferred to a PVDF membrane, as previously described[41]. The membrane was probed with anti-V5, anti-human NMNAT1 (1:500; Novus Biologicals) or β-actin (Santa Cruz Biotechnology) followed by IRDye (LI-COR) goat anti-mouse IgG and antibody binding detected with an Odyssey infrared imager (LI-COR).

Recombinant protein production and purification

Human *NMNAT1* cDNA was amplified by reverse transcription polymerase chain reaction (RT-PCR) from a cDNA clone (OpenBiosystem), cloned into a pENTR/D-TOPO entry vector (Invitrogen), and fully sequence-verified. The coding sequence was moved by recombination to a Gateway compatible destination expression vector modified to contain N-terminal V5 (pCAG-V5-IRES-EGFP) or Flag (pCAG-Flag-IRES-EGFP) epitope tags in frame. Plasmid DNA was purified using the EndoFree plasmid maxi kit (Qiagen). Recombinant NMNAT1 (with Flag-tag) expressed in CHO cells was purified using a FLAG M Purification kit (Sigma) for subsequent enzyme activity assay.

NIH-PA Author Manuscript

NIH-PA Author Manuscript

NIH-PA Author Manuscript

NMNAT enzyme activity assay

NMNAT activity was measured by high performance liquid chromatography (HPLC) quantitation of the reaction product, NAD^+. The assay mixture contained 1.5 mM ATP, 1 mM nicotinamide mononucleotide (NMN), 10 mM $MgCl_2$ in 25 mM Tris-HCl (pH 7.4), and the appropriate amount of enzyme sample (typically, 20 or 40 μL) to achieve a final volume of 0.2 mL. The reaction was started by the addition of the substrate NMN. After incubation for 10, 30, or 120 min at 37 °C, a 40 μL aliquot of the reaction mixture was withdrawn and added to 20 μL of ice-cold 1.2 M PCA containing 20 mM EDTA and 0.15% sodium metabisulfite to stop the reaction. After a 15 min incubation at 4°C, the mixture was centrifuged for 10 min at 16,000 × g in a Beckman microcentrifuge. A 55 μL aliquot of the supernatant was further neutralized by the addition of 20 μL of ice-cold 1 M K_2CO_3 and centrifuged again. The supernatant was isolated and stored at −80°C until HPLC analysis.

Sample preparation for HPLC analyses of NAD^+

Harvested cells were rinsed with Hank's balanced salt solution twice and centrifuged at 2,150 × g for 5 min. The cell pellet was resuspended with argon-bubbled 20 mM Tris-HCl pH 7.4 for analysis of the oxidized dinucleotides including NAD^+. The cell suspension was extracted with 4 volumes of argon-bubbled ice-cold 1.2M perchloric acid (PCA) containing 20 mM EDTA and 0.15% sodium metabisulfite. After vortexing, the suspension was placed on ice for 15 minutes and then centrifuged at 16,000 × g for 10 min. The supernatant was neutralized with 1 M potassium carbonate and centrifuged to remove insoluble material. The pellet from the PCA extraction was used for protein estimation. Samples were stored at −80°C and subjected to HPLC analysis.

HPLC conditions for analyses of NAD^+

Separation of the oxidized dinucleotides was carried out on a C18 column (5 μm, 4.6 × 250 mm, Adsorbosphere XL C18 90Å) preceded by a guard column at 40°C. Flow rate was set at 0.5 mL/min. The mobile phase was initially 100% of mobile phase A (0.1 M sodium phosphate buffer, pH 6.0, containing 3.75% methanol). The methanol was linearly increased with mobile phase B (0.1 M sodium phosphate buffer, pH 6.0, containing 30% methanol), increasing to 50% over 15 minutes. The column was washed after each separation by increasing mobile phase B to 100% for 5 min. UV absorbance was monitored at 260 and 340 nm with Shimadzu SPD-M20A. Pertinent peak areas were integrated by the LabSolution software from Shimadzu, and quantified using standard curves.

Statistical analyses

For comparison of activity rates of purified, recombinant NMNAT1 proteins relative to wild-type, rates were normalized by the mean rate of the wild-type protein analyzed on the same day to account for variation in the absolute enzyme activity rates on different analysis dates. The significance of group differences was evaluated using a non-parametric Wilcoxon rank sum test in SAS 4.3 due to skewness observed in the data and small sample size. For measurements of cellular NMNAT activity and NAD^+ levels, statistical comparisons between groups were performed using Student's 2-tailed *t*-test.

Supplementary Material

Refer to Web version on PubMed Central for supplementary material.

Acknowledgments

We thank Maria Sousa, Daniel Harnley, Marie-Elise Lancelot and Aline Antonio for their excellent technical assistance, The Children's Hospital of Philadelphia CytoGenomics laboratory for assistance with fibroblast cell line

NIH-PA Author Manuscript

NIH-PA Author Manuscript

NIH-PA Author Manuscript

establishment and culture, and Joseph Baur for his helpful discussions on NAD^+ metabolism. We are grateful to the patients and their relatives for their participation in this study.

This work was supported by grants from the National Institutes of Health (RO1-EY12910 (E.A.P.), R03-DK082446 (M.J.F.), R01-GM097409 (E.N.-O.), P30HD026979 (M.J.F., R.X.) and P30EY014104 (MEEI core support)); the Foundation Fighting Blindness USA (I.A., A.D.B., E.L.B., S.S.B., Q.L., A.T.M., D.S.M., E.A.P., J.-A.S., S.M.-S., A.R.W.); Rosanne Silbermann Foundation (E.A.P.); Penn Genome Frontiers Institute (E.A.P, X.G.); Institutional Fund to the Center for Biomedical Informatics by the Loyola University Stritch School of Medicine (X.G.); the Foerderer Award for Excellence from the Children's Hospital of Philadelphia (M.J.F., X.G.); The Angelina Foundation Fund from the Division of Rehabilitation and Metabolic Disease at The Children's Hospital of Philadelphia (M.J.F.); The Clinical and Translational Research Center at The Children's Hospital of Philadelphia (UL1-RR-024134) (M.J.F., E.A.P.); the Department of Biotechnology, Government of India and the Champalimaud Foundation, Portugal (C.K.); the Hyderabad Eye Research Foundation (C.K.); a senior research fellowship from the Council for Scientific and Industrial Research (R.S.); Foundation Voir et Entendre (C.Z.), Ville de Paris and Région Ille de France; RP Fighting Blindness (UK)(A.R.W.), Fight For Sight (UK) (A.D.B., S.S.B., A.T.M., D.S.M., A.R.W.), Moorfields Eye Hospital NIHR BRC for Ophthalmology (A.D.B., S.S.B., A.T.M., D.S.M., A.R.W.), Special Trustees of Moorfields Eye Hospital (A.D.B., S.S.B., A.T.M., D.S.M., A.R.W.). The content is solely the responsibility of the authors and does not necessarily represent the official views of the funding organizations or the National Institutes of Health.

REFERENCES

1. Weleber RG. Infantile and childhood retinal blindness: a molecular perspective. Ophthalmic Genet. 2002:71–97. [PubMed: 12187427]
2. Michaelides M, Hardcastle AJ, Hunt DM, Moore AT. Progressive cone and cone-rod dystrophies: phenotypes and underlying molecular genetic basis. Survey of Ophthalmology. 2006; 51:232–258. [PubMed: 16644365]
3. den Hollander AI, Black A, Bennett J, Cremers FP. Lighting a candle in the dark: advances in genetics and gene therapy of recessive retinal dystrophies. J. Clin. Invest. 2010; 120:3042–3053. [PubMed: 20811160]
4. Keen TJ, et al. Identification of a locus (LCA9) for Leber's congenital amaurosis on chromosome 1p36. Eur. J. Hum. Genet. 2003; 11:420–423. [PubMed: 12734549]
5. Lau C, Niere M, Ziegler M. The NMN/NaMN adenylyltransferase (NMNAT) protein family. Front. Biosci. 2009; 14:410–431. [PubMed: 19273075]
6. Pierce EA. Pathways to photoreceptor cell death in inherited retinal degenerations. Bioessays. 2001; 23:605–618. [PubMed: 11462214]
7. Daiger SP, Bowne SJ, Sullivan LS. Perspective on genes and mutations causing retinitis pigmentosa. Arch. Ophthalmol. 2007; 125:151–158. [PubMed: 17296890]
8. Maguire AM, et al. Safety and efficacy of gene transfer for Leber's congenital amaurosis. N. Engl. J. Med. 2008; 358:2240–2248. [PubMed: 18441370]
9. Bainbridge JW, et al. Effect of gene therapy on visual function in Leber's congenital amaurosis. N. Engl. J. Med. 2008; 358:2231–2239. [PubMed: 18441371]
10. Cideciyan AV, et al. Human gene therapy for RPE65 isomerase deficiency activates the retinoid cycle of vision but with slow rod kinetics. Proc. Natl. Acad. Sci. USA. 2008; 105:15112–15117. [PubMed: 18809924]
11. Maguire AM, et al. Age-dependent effects of *RPE65* gene therapy for Leber's congenital amaurosis: a phase 1 dose-escalation trial. Lancet. 2009; 374:1597–1605. [PubMed: 19854499]
12. Jacobson SG, et al. Gene therapy for Leber congenital amaurosis caused by RPE65 mutations: safety and efficacy in 15 children and adults followed up to 3 years. Arch. Ophthalmol. 2012; 130:9–24. [PubMed: 21911650]
13. Sherry ST, et al. dbSNP: the NCBI database of genetic variation. Nucleic Acids Res. 2001; 29:308–311. [PubMed: 11125122]
14. 1000 Genomes Project Consortium. A map of human genome variation from population-scale sequencing. Nature. 2010; 467:1061–1073. [PubMed: 20981092]
15. Grant GR, et al. Comparative analysis of RNA-Seq alignment algorithms and the RNA-Seq unified mapper (RUM). Bioinformatics. 2011; 27:2518–2528. [PubMed: 21775302]

NIH-PA Author Manuscript

NIH-PA Author Manuscript

NIH-PA Author Manuscript

16. Ramensky V, Bork P, Sunyaev S. Human non-synonymous SNPs: server and survey. Nucleic Acids Res. 2002; 30:3894–3900. [PubMed: 12202775]
17. Ng PC, Henikoff S. SIFT: Predicting amino acid changes that affect protein function. Nucleic Acids Res. 2003; 31:3812–3814. [PubMed: 12824425]
18. Sullivan LS, et al. Prevalence of disease-causing mutations in families with autosomal dominant retinitis pigmentosa: a screen of known genes in 200 families. Invest. Ophthalmol. Vis. Sci. 2006; 47:3052–3064. [PubMed: 16799052]
19. Stone EM. Leber congenital amaurosis - a model for efficient genetic testing of heterogeneous disorders: LXIV Edward Jackson Memorial Lecture. Am. J. Ophthalmol. 2007; 144:791–811. [PubMed: 17964524]
20. Wang M, Marin A. Characterization and prediction of alternative splice sites. Gene. 2006; 366:219–227. [PubMed: 16226402]
21. Belenky P, Bogan KL, Brenner C. NAD+ metabolism in health and disease. Trends Biochem. Sci. 2007; 32:12–19. [PubMed: 17161604]
22. Berger F, Lau C, Dahlmann M, Ziegler M. Subcellular compartmentation and differential catalytic properties of the three human nicotinamide mononucleotide adenylyltransferase isoforms. J. Biol. Chem. 2005; 280:36334–36341. [PubMed: 16118205]
23. Coleman MP, Freeman MR. Wallerian degeneration, wld(s), and nmnat. Ann. Rev. Neurosci. 2010; 33:245–267. [PubMed: 20345246]
24. Conforti L, et al. Reducing expression of NAD+ synthesizing enzyme NMNAT1 does not affect the rate of Wallerian degeneration. FEBS J. 2011; 278:2666–2679. [PubMed: 21615689]
25. Zhai RG, et al. Drosophila NMNAT maintains neural integrity independent of its NAD synthesis activity. PLoS Biol. 2006; 4:e416. [PubMed: 17132048]
26. Siepel A. Evolutionarily conserved elements in vertebrate, insect, worm, and yeast genomes. Genome Res. 2005; 15:1034–1050. [PubMed: 16024819]
27. Worth CL, Preissner R, Blundell TL. SDM—a server for predicting effects of mutations on protein stability and malfunction. Nucleic Acids Res. 2011; 39:W215–W222. [PubMed: 21593128]
28. Bogan KL, Brenner C. Nicotinic acid, nicotinamide, and nicotinamide riboside: a molecular evaluation of NAD+ precursor vitamins in human nutrition. Ann. Rev. Nutrit. 2008; 28:115–130. [PubMed: 18429699]
29. Nikiforov A, Dolle C, Niere M, Ziegler M. Pathways and subcellular compartmentation of NAD biosynthesis in human cells: from entry of extracellular precursors to mitochondrial NAD generation. J. Biol. Chem. 2011; 286:21767–21778. [PubMed: 21504897]
30. Conforti L, et al. Wld S protein requires Nmnat activity and a short N-terminal sequence to protect axons in mice. J. Cell Biol. 2009; 184:491–500. [PubMed: 19237596]
31. Avery MA, Sheehan AE, Kerr KS, Wang J, Freeman MR. Wld S requires Nmnat1 enzymatic activity and N16-VCP interactions to suppress Wallerian degeneration. J. Cell Biol. 2009; 184:501–513. [PubMed: 19237597]
32. Berger F, Lau C, Ziegler M. Regulation of poly(ADP-ribose) polymerase 1 activity by the phosphorylation state of the nuclear NAD biosynthetic enzyme NMN adenylyl transferase 1. Proc. Natl. Acad. Sci. USA. 2007; 104:3765–3770. [PubMed: 17360427]
33. den Hollander AI, Roepman R, Koenekoop RK, Cremers FP. Leber congenital amaurosis: genes, proteins and disease mechanisms. Prog. Retin. Eye Res. 2008; 27:391–419. [PubMed: 18632300]
34. Chun S, Fay JC. Identification of deleterious mutations within three human genomes. Genome Res. 2009; 19:1553–1561. [PubMed: 19602639]
35. Wei Q, Wang L, Wang Q, Kruger WD, Dunbrack RL Jr. Testing computational prediction of missense mutation phenotypes: functional characterization of 204 mutations of human cystathionine beta synthase. Proteins. 2010; 78:2058–2074. [PubMed: 20455263]
36. Gnirke A, et al. Solution hybrid selection with ultra-long oligonucleotides for massively parallel targeted sequencing. Nat. Biotechnol. 2009; 27:182–189. [PubMed: 19182786]
37. Li H, Durbin R. Fast and accurate short read alignment with Burrows-Wheeler transform. Bioinformatics. 2009; 25:1754–1760. [PubMed: 19451168]

NIH-PA Author Manuscript

NIH-PA Author Manuscript

NIH-PA Author Manuscript

38. Li H, et al. The Sequence Alignment/Map format and SAMtools. Bioinformatics. 2009; 25:2078–2079. [PubMed: 19505943]

39. Benjamini Y, Hochberg Y. Controlling the false discovery rate: a practical and powerful approach to multiple testing. J. Royal Stat. Soc. B (Methodological). 1995; 57:289–300.

40. Liu Q, Zuo J, Pierce EA. The retinitis pigmentosa 1 protein is a photoreceptor microtubule-associated protein. J. Neurosci. 2004; 24:6427–6436. [PubMed: 15269252]

41. Davis EE, et al. *TTC21B* contributes both causal and modifying alleles across the ciliopathy spectrum. Nat. Genet. 2011; 43:189–196. [PubMed: 21258341]

NIH-PA Author Manuscript
NIH-PA Author Manuscript
NIH-PA Author Manuscript

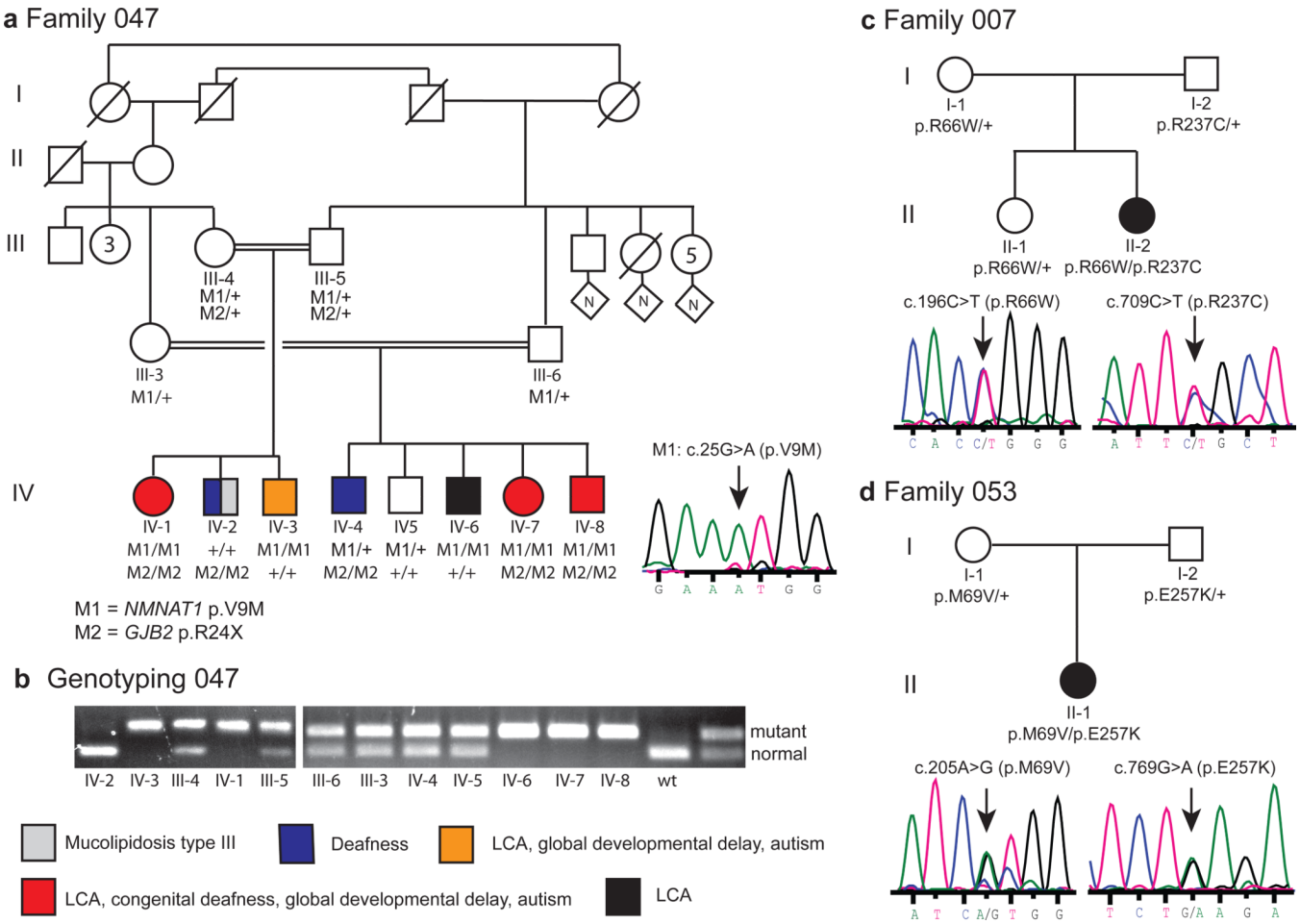

Figure 1.

Pedigrees of three LCA kindreds evaluated at The Children's Hospital of Philadelphia in whom mutations were identified in *NMNAT1*. (**a**) Family 047. Consanguineous Pakistani kindred in which homozygous *NMNAT1* mutations were identified in five children with LCA by whole exome sequencing with Sanger sequencing validation. M1 = *NMNAT1* mutation (c.25G>A, p.Val9Met). M2 = *GJB2* mutation (c.71G>A , p.Trp24*). A representative sequence trace for the M1 mutation is shown. Exome sequencing confirmed the presence of the p.Trp24* homozygous mutation in *GJB2* in the two children (IV-1 and IV-2) who were affected with sensorineural hearing loss. Sanger sequencing verified that this mutation also segregated with the hearing loss phenotype in their larger kindred. Subject IV-2 had no identifiable pathogenic mutations within any of the known mucolipidosis disease genes. (**b**) The members of family 047 were genotyped by PCR amplification of exon 2 of *NMNAT1*, followed by digestion of the PCR products with AcuI to distinguish the wild-type from the mutant sequence. The genotyping data illustrate the segregation of the mutant *NMNAT1* (M1) allele only in the five children with LCA in generation IV, whereas the four unaffected parents of these children in generation III carry both the mutant and wild-type alleles, and their three children with normal vision harbor only the wild-type allele. Individuals III-4, III-5, IV-1, IV-2 and IV-3 were clinically evaluated by M.J.F. and E.A.P.; individuals III-3, III-6 and V-4 to IV-7 were not clinically evaluated by the authors. (**c**) Family 007. A single LCA proband was identified by Sanger sequencing of *NMNAT1* to harbor compound heterozygous mutations c.196C>T (p.Arg66Trp) and c.709C>T (p.Arg237Cys). (**d**) Family 053. A single LCA proband was identified by Sanger sequencing of

NIH-PA Author Manuscript

NIH-PA Author Manuscript

NIH-PA Author Manuscript

NMNAT1 to harbor compound heterozygous mutations c.205A>G (p.Met69Val) and c. 769G>A (p.Glu257Lys). The '+' or 'M' below each symbol represents a wild-type or specific mutant allele. Squares and circles indicate male or female, respectively, and numbers within symbols indicate multiple offspring of a given gender. Slashes depict deceased individuals. Colors within symbols indicate affected individuals, with phenotypes defined in the pedigree key.

NIH-PA Author Manuscript

NIH-PA Author Manuscript

NIH-PA Author Manuscript

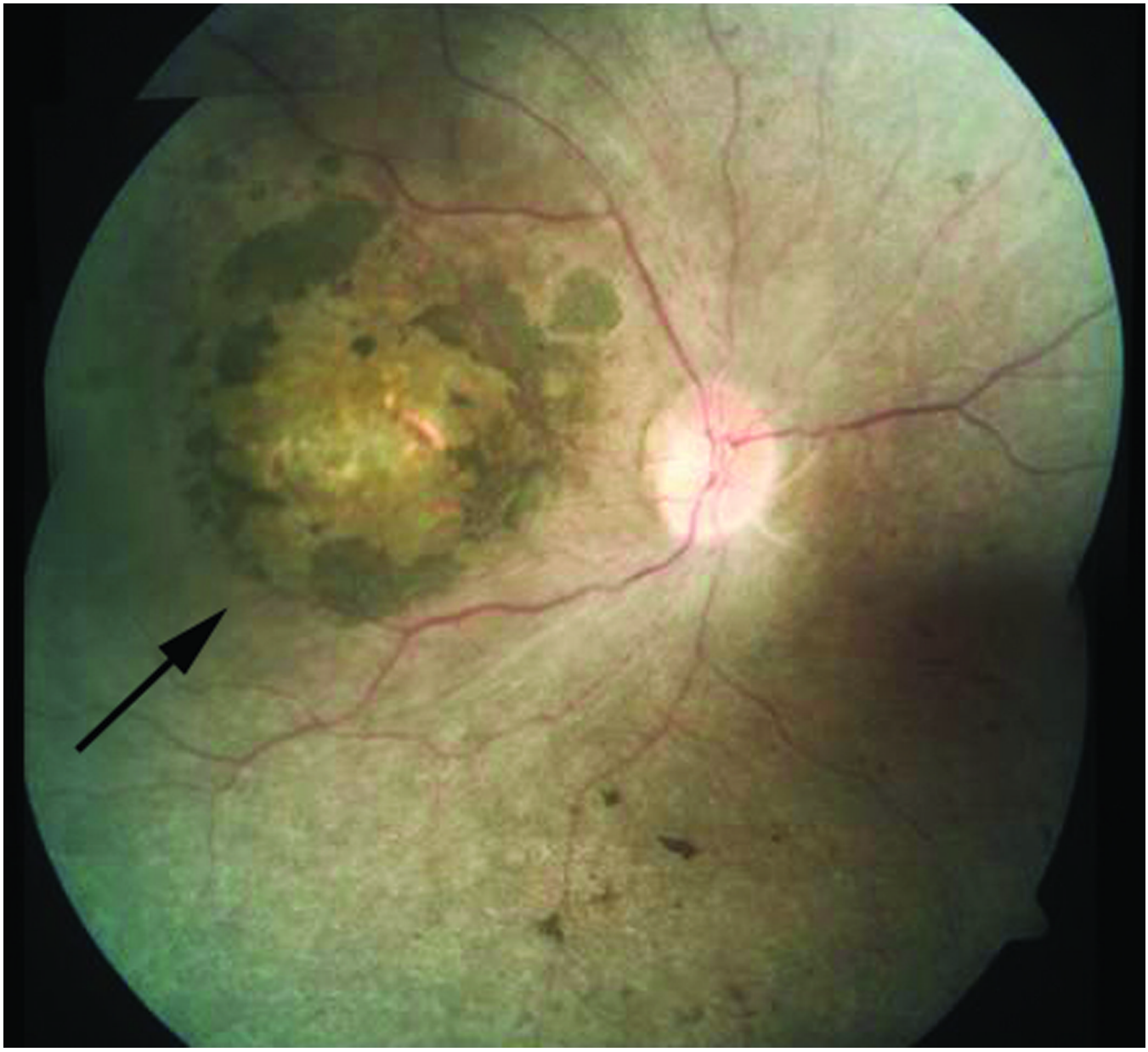

Figure 2.

Retinal image from individual with LCA due to mutations in *NMNAT1*. Composite fundus image of the right eye of subject II-1, LVPEI family LCA-100, showing pallor of the optic disc, attenuation of the retinal blood vessels, pigment disruption and atrophic changes in the macula (arrow), and scattered pigment clumping in the peripheral retina. The optic disc is approximately 1.75 mm in diameter.

NIH-PA Author Manuscript
NIH-PA Author Manuscript
NIH-PA Author Manuscript

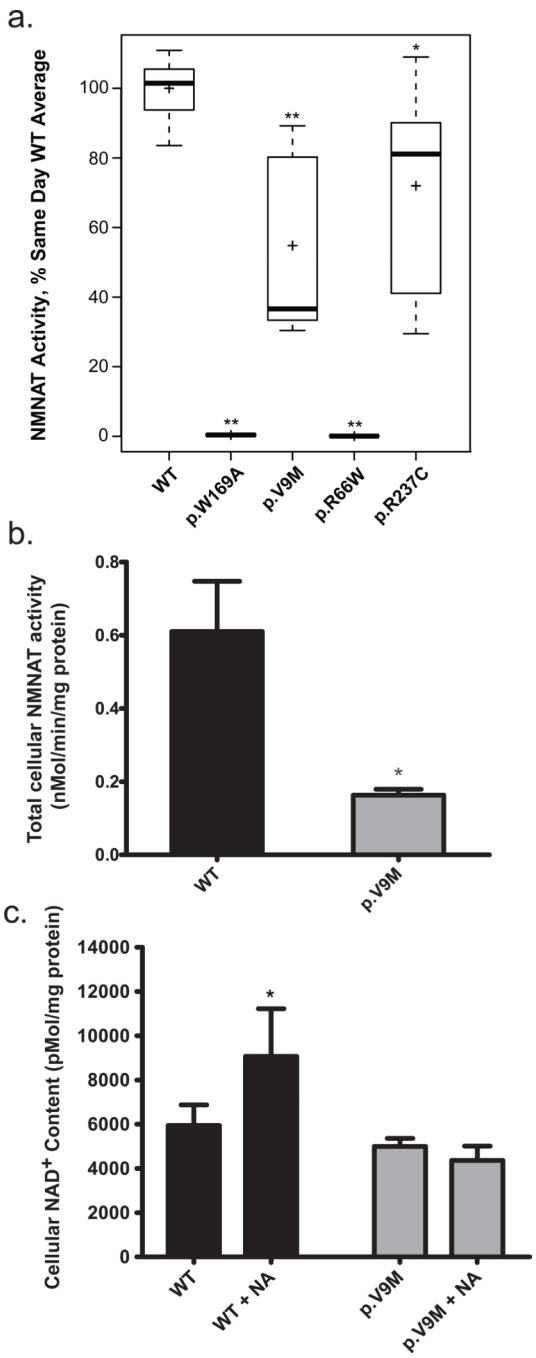

Figure 3.

NMNAT1 enzyme activity and cellular NAD^+ content. (**a**) The NAD^+ biosynthetic activity of wild-type, p.Val9Met, p.Arg66Trp, p.Arg237Cys and p.Trp169Ala purified recombinant NMNAT1 proteins was measured as described. Boxplots display activity measurements of independently generated and measured replicate protein preparations. The length of the box represents 25^{th} to 75^{th} inter-quartile range, the interior horizontal line represents the median, the interior cross represents the mean, and vertical lines issuing from the box extend to the minimum and maximum values of the analysis variable. The p.Trp169Ala mutant had complete loss of NMNAT1 enzyme activity ($n = 6$; $P = 0.0014$), as was previously reported[32]. The p.Val9Met mutant protein NMNAT1 enzyme activity was significantly

NIH-PA Author Manuscript

NIH-PA Author Manuscript

NIH-PA Author Manuscript

reduced at 37% of wild-type control ($n = 7$; $P = 0.0015$). The p.Arg237Cys mutant protein showed an average of 81% of wild-type NMNAT1 activity ($n = 6$; $P = 0.034$). The p.Arg66Trp mutant protein showed complete loss of enzyme activity ($n = 6$; $P = 0.0014$), although we were not able to achieve effective purification of the Flag-tagged version of the p.Arg66Trp mutant protein (Supplementary Fig. 6) despite its clearly normal expression and nuclear localization in CHO and IMCD3 cells (Supplementary Fig. 5). Further experiments will be needed to determine if the Flag-tagged p.Arg66Trp protein is unstable to purification. *$P < 0.05$ and **$P < 0.01$ determined by non-parametric Wilcoxon rank sum test. (**b**) Total cellular NMNAT enzyme activity was measured in whole cell extracts of fibroblasts from a healthy control and the LCA proband from Family 047 (subject IV-1) who was homozygous for the p.Val9Met NMNAT1 variant. The p.Val9Met mutant cells had 27% of total cellular NMNAT NAD^+ synthetic activity relative to control cells (two-tailed *t* test $P = 0.016$; $n = 6$ for wild-type, $n = 5$ for LCA proband cells). (**c**) Cellular NAD^+ levels. Total cellular NAD^+ content was quantified by HPLC in control and LCA proband IV-1 (Fig. 1a) fibroblasts at baseline and following 10 mM nicotinic acid treatment for 24 hours. NAD^+ content in fibroblast cells from the LCA proband (p.Val9Met) was decreased by 16% relative to those from a wild-type control ($P = 0.067$). Nicotinic acid treatment significantly increased NAD^+ content in control cells ($P < 0.05$) but had no effect on NAD^+ content in the proband's cells ($P > 0.05$). $n = 7$ for both cell lines without treatment, $n = 6$ for control cells treated with nicotinic acid, and $n = 4$ for IV-1 cells treated with nicotinic acid. For **b** and **c**, bars indicate mean and standard error. *$P < 0.05$.

NIH-PA Author Manuscript
NIH-PA Author Manuscript
NIH-PA Author Manuscript

Table 1

Summary of identified *NMNAT1* mutations

	Ethnicity/ nationality	Mutations		EVS	PolyPhen2[a]	SIFT[b]
CHOP/MEEI						
LCA-047	Pakistan	c.25G>A	p.Val9Met (homo)	Novel	PoD	D
LCA-007	Asian American	c.196C>T c.709C>T	p.Arg66Trp p.Arg237Cys	Novel 1/7,019	PrD PrD	D D
LCA-053	African American	c.205A>G c.769G>A	p.Met69Val p.Glu257Lys[c]	Novel 13/10,745	PrD B	D T
LVPEI						
LCA-73	Indian	c.25G>A	p.Val9Met (homo)	Novel	PoD	D
LCA-79	Indian	c.98A>G	p.Asp33Gly (homo)	Novel	PrD	D
LCA-100	Indian	c.709C>T c.565delG	p.Arg237Cys p.Ala189Leufs*25	1/7,019 Novel	PrD	D
LCA-128	Indian	c.215T>A	p.Leu72His (homo)	Novel	PrD	D
UCL						
LCA-1	European descent	c.205A>G c.769G>A	p.Met69Val p.Glu257Lys	Novel 13/10,745	PrD B	D T
LCA-2	Caribbean, Sri Lankan	c.161C>T c.293T>G	p.Ala54Val p.Val98Gly	1/10,757 Novel	PrD PrD	D T
LCA-3	Caribbean	c.37G>A c.293T>G	p.Ala13Thr p.Val98Gly	1/10,757 11/10,747	PrD PrD	D T
LCA-4	Caribbean, Irish	c.723delA c.769G>A	p.Pro241Profs*45 p.Glu257Lys	Novel 13/10,745	N/A B	N/A T
LCA-5	Polish	c.59T>A c.769G>A	p.Ile20Asn p.Glu257Lys	Novel 13/10,745	PrD B	D T
LCA-6	British Caucasian	c.552A>G c.769G>A	p.Ile184Met p.Glu257Lys	Novel 13/10,745	PoD B	D T
LCA-7	British Caucasian	c.466G>C c.769G>A	p.Gly156Arg p.Glu257Lys	Novel 13/10,745	PrD B	D T

[a] PolyPhen2: Hum-Var score PrD, probably damaging; PoD, possibly damaging; B, benign.

[b] SIFT: D, damaging; T, tolerated.

NIH-PA Author Manuscript
NIH-PA Author Manuscript
NIH-PA Author Manuscript

[c]The p.Glu257Lys variant in NMNAT1 was detected in a total of six families. While this variant is sufficiently rare to be associated with LCA (estimated prevalence of 1:30,000) [33] based on ESP data (13/10745 = 0.12%), it is not predicted to damage protein function by PolyPhen2 or SIFT. However, it is known that these prediction programs have significant false positive and negative rates and frequently do not agree with one another[34,35] We therefore employed Fisher's exact test to estimate the probability that the p.Glu257Lys variant causes disease. The results of this analysis showed the allele frequency for the p.Glu257Lys variant was significantly higher in the LCA cases (6/568 chromosomes = 1.056%) compared to both our controls (0/1,002 chromosomes = 0%; $P = 0.002$) and ESP samples (13/10,758 chromosomes = 0.121%; $P = 0.0002$), which is consistent with a high likelihood that this variant is pathogenic. Future empiric studies of the effect of this mutation on protein function, both alone and in combination with the observed series of compound heterozygous partner alleles, will be needed to validate the pathogenicity of this NMNAT1 variant.